

Preparation of a Homogeneously Dispersed BaTiO₃/Polymer Nanocomposite Thin Film

David E. Collins and Elliott B. Slamovich*

School of Materials Engineering, Purdue University,
W. Lafayette, Indiana 47907

Received June 2, 1999

Revised Manuscript Received July 29, 1999

Studies to process BaTiO₃/polymer composites for dielectric applications have focused on conventional compounding techniques that entail mixing micrometer-scale BaTiO₃ powders with either a polymer–solvent solution¹ or a polymer melt.² These methods are generally limited by powder coagulation and are not amenable to processing thin films. An alternative approach involves the use of chemical–solution methods in which crystalline BaTiO₃ is precipitated from the reaction of a titanium alkoxide and Ba(OH)₂. Precursors to BaTiO₃/polymer composites may be processed by mixing a titanium alkoxide and a polymer in a common solvent. The low viscosity of the precursor solution facilitates thin film deposition methods including spin casting, dipping, or spray casting. After solvent removal, the titanium alkoxide is converted to BaTiO₃ by reacting the films below 100 °C in aqueous alkaline solutions containing barium.³ This approach does not ensure a homogeneous dispersion of BaTiO₃ particles, and a segregated composite microstructure will develop if the titanium alkoxide and polymer, although soluble in a common solvent, are immiscible in one another.^{4–6} Immiscibility has been minimized in hybrid materials by covalently bonding a metal alkoxide with the polymer matrix to form monolithic materials.^{7–11} This approach is extended here to increase the dispersion of BaTiO₃ in a polymer matrix.

BaTiO₃/polymer thin films were prepared from solutions of titanium diisopropoxide bis(ethylacetoacetate) (TIBE)¹² dissolved in toluene with either a polystyrene-block-polybutadiene-block-polystyrene (SBS)¹³ or polystyrene-co-maleic anhydride (~14 wt % maleic anhydride, (S-MAH))¹⁴ block copolymer. The volume fraction

of BaTiO₃ in the final composite was controlled by varying the relative weight fraction of the TIBE to SBS or S-MAH in the precursor solution. TIBE/SBS precursor films were prepared from solutions containing 0.04 w/v SBS/toluene while TIBE/S-MAH films were cast from solutions diluted to 0.02 w/v S-MAH/toluene. Uniform TIBE/polymer precursor films of thickness < 1 μm were achieved by depositing the precursor solution onto Ag-coated polycarbonate substrates using a 0.22-μm glass filter syringe, and spin casting at 8000 rpm for 20 s. After the films were dried in a desiccator for 12 h, the precursor films were reacted in aqueous solutions of 1.0 M Ba(OH)₂ at 80 °C for 1 h.^{6,15,16} To minimize the formation of BaCO₃ on the film surface upon removal from the Ba(OH)₂ solution, the films were washed with hot water (pH > 10) and subsequently rinsed with ethanol. Cross sections of the films sufficiently thin for transmission electron microscopy (TEM) were prepared by ultramicrotomy.¹⁷

BaTiO₃/SBS films prepared from precursor solutions containing 90 wt % TIBE relative to SBS exhibited a bilayer structure. On the film surface, a continuous layer of BaTiO₃ covered an interior composite layer composed of regions rich in BaTiO₃ nanoparticles (~5 nm) distributed throughout the SBS matrix (Figure 1a). Powder X-ray diffraction of the film indicated that the BaTiO₃ particles were crystalline.³ This segregated morphology was a result of segregation between TIBE and SBS that occurred in the precursor solution, or during drying after spin casting. Energy dispersive spectroscopy performed on microtomed sections of the TIBE/SBS precursor film showed that the spin-cast film segregated into titanium-rich and titanium-poor regions.⁶ Segregation also was observed in solutions using the homopolymers, polystyrene, and polybutadiene.¹⁸

As with the BaTiO₃/SBS film, the BaTiO₃/S-MAH film prepared from 90 wt % TIBE solution exhibited a continuous layer of BaTiO₃ on the film surface (Figure 1b). However, the interior composite layer consisted of a uniform dispersion of BaTiO₃ nanoparticles throughout the S-MAH matrix. Again, powder X-ray diffraction indicated that the BaTiO₃ particles were crystalline. Further, the microtomed sections exhibited sharp electron diffraction rings in the TEM, indicating that the particles were nanocrystalline BaTiO₃. The vertical cracks in the film were a product of ultramicrotomy, and the arch running horizontally across the section is discussed below. The improved dispersion of BaTiO₃ may be explained via bonding between the TIBE and maleic anhydride (MAH) groups in S-MAH, much like

* To whom all correspondence should be addressed.

(1) Gregorio, R., Jr.; Cestari, M.; Bernardino, F. E. *J. Mater. Sci.* **1996**, *31*, 2925–2930.

(2) Aulagner, E.; Guillet, J.; Seytre, G.; Hantouche, C.; Le Gonidec, P.; Terzulli, G. *IEEE 5th International Conference on Conduction and Breakdown in Solid Dielectrics* **1995**, 423–427.

(3) Collins, D. E.; Slamovich, E. B. *Mater. Res. Symp. Proc.*; Komarneni, S., Parker, J., Wollenberger, H., Eds. **1997**, *457*, 445–50.

(4) Embs, F. W.; Thomas, E. L.; Wung, C. J.; Prasad, P. N. *Polymer* **1993**, *34*, 4607–4612.

(5) Burdon, J. W.; Calvert, P. *Mater. Res. Soc. Symp.*; Alper, M., Ed. **1991**, *218*, 203–212.

(6) Collins, D. E.; Slamovich, E. B. Submitted to the *J. Mater. Res.*

(7) Novak, B. *Adv. Mater.* **1993**, *5*, 422–433.

(8) Yoshinaga, I.; Katayama, S. *J. Sol-Gel Sci. Technol.* **1996**, *6*, 151–154.

(9) Wei, Y.; Bakthavatchalam, R.; Whitecar, C. K. *Chem. Mater.* **1990**, *2*, 337–339.

(10) Huang, Z. H.; Dong, J. H.; Aiu, K. Y.; Wei, Y. *J. Appl. Polym. Sci.* **1997**, *66*, 853–860.

(11) Nass, R.; Schmidt, H.; Arpac, E. In *Sol-Gel Optics, Proc. SPIE* **1990**, *1328*, 258–63.

(12) Gelest Chemical Company, Tullytown, PA.

(13) Kraton D1102, Shell Chemical Company, Baytown, TX.

(14) Aldrich, Milwaukee, WI.

(15) Lencka, M. M.; Riman, R. E. *Chem. Mater.* **1993**, *5*, 61–70.

(16) Slamovich, E. B.; Aksay, I. A. *Mater. Res. Soc. Symp. Proc.* Cheetham, A. K., Ed. **1994**, *346*, 63–68.

(17) Ultramicrotomy samples were embedded in Epo-Fix embedding media (Electron Microscopy Sciences, Ft. Washington, PA) and sectioned on a Reichert-Jung Ultracut E at 1 mm/s using a 55° diamond knife.

(18) Segregation was determined by energy dispersive spectroscopy on samples prepared by spin casting the precursor solution directly onto 200-mesh, TEM grids. Using a precursor solution that was diluted with toluene to a 0.01 w/v polymer/toluene solution, this process produced a thickness gradient such that the film centers on the grid were electron-transparent.

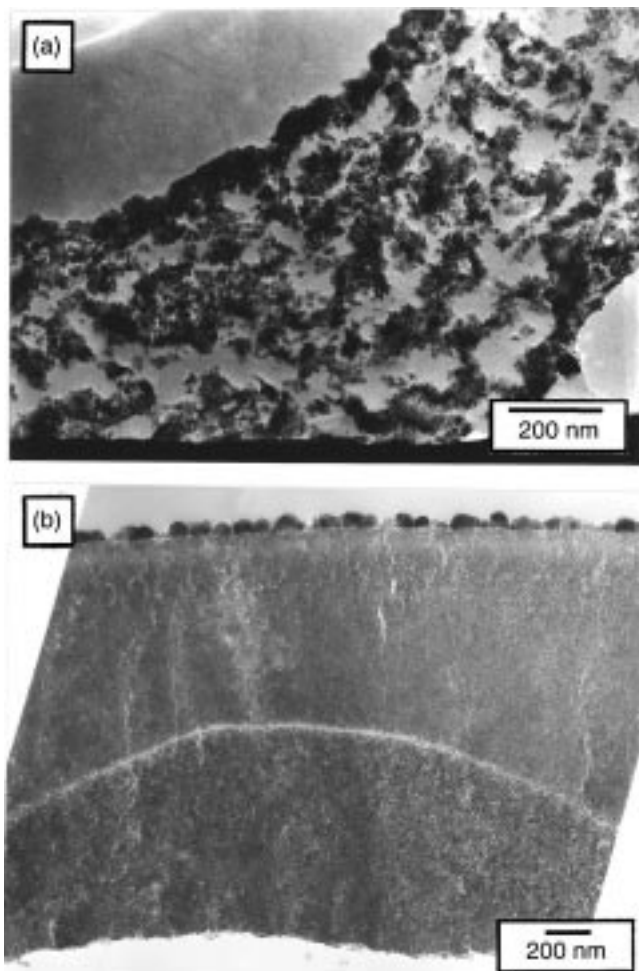


Figure 1. Thin-film cross sections of (a) BaTiO₃/SBS and (b) BaTiO₃/S-MAH composites prepared from precursor solutions containing 90 wt % TIBE and reacted at 80 °C for 1 h in 1.0 M Ba(OH)₂.

methacrylic acid has been used to bind compounds of zirconium^{11,19} or zinc.²⁰ In this case, bound TIBE alters the functionality of the MAH block such that the miscibility between unbound TIBE and the S-MAH increases.

The reaction between TIBE and MAH was examined using Fourier transform infrared spectroscopy (FTIR). A TIBE/S-MAH precursor solution was prepared by mixing 80 wt % TIBE relative to S-MAH in 0.04 w/v S-MAH/toluene. This composition was chosen because specific peaks from both TIBE and S-MAH materials could be observed. The TIBE/S-MAH solution gelled after 48 h at room temperature. FTIR was performed in transmittance on samples of the TIBE/S-MAH solution sandwiched between NaCl plates before and after gelation (Figure 2). The spectra of the starting materials are shown also for comparison, and as expected, most

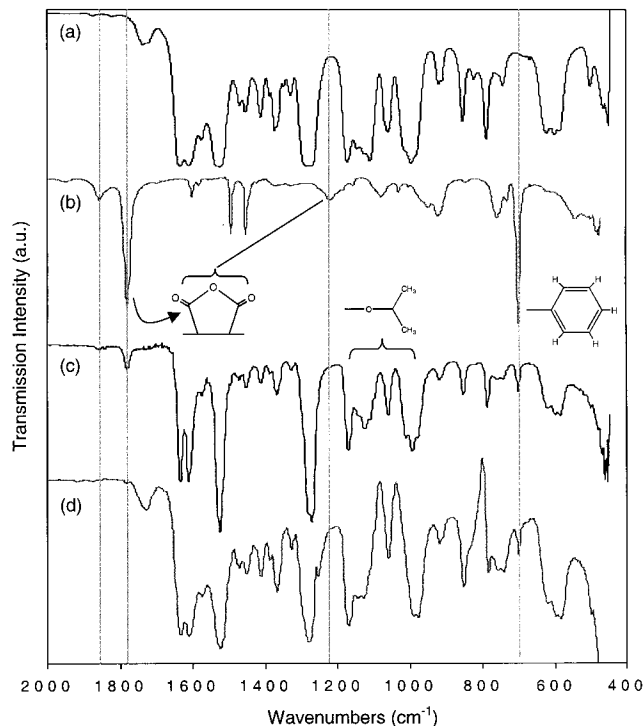


Figure 2. FTIR spectra of pure (a) TIBE and (b) S-MAH as well as the 80/20 TIBE/S-MAH precursor gel formation (c) before and (d) after gel formation. Lines indicate peaks associated with S-MAH. Molecular structures are included to depict relevant functional groups.

of the peaks observed in the 80/20 TIBE/S-MAH spectrum are associated with TIBE due to its higher concentration. The C–H peak ascribed to the phenyl ring of polystyrene (located at 700 cm⁻¹) was used as an internal standard because it did not react with TIBE.

The spectrum taken before the precursor gelled contained the cyclic anhydride carbonyl peaks (1855 and 1780 cm⁻¹), indicating that at least some of the anhydride did not react shortly after mixing the TIBE and S-MAH. Although the anhydride peak corresponding to the C–O–C bond at 1220 cm⁻¹ was present, it was almost completely masked by TIBE absorptions. After the precursor gelled, peaks associated with the anhydride carbonyls were replaced by a new peak at 1730 cm⁻¹, a wavenumber region commonly associated with carbonyl stretching of acids, esters, and normal anhydrides. In addition, changes in peak shape and intensity were observed in the peaks originating from C–O stretching (1020–975 cm⁻¹) and –CH₃ bending (1170–1130 cm⁻¹) of the isopropoxide groups.²¹ How these changes relate to the gel structure is unclear, but it does imply these ligands participate in the reaction. In contrast, peaks associated with ethyl acetoacetate^{21,22} do not undergo significant change.

From these results, a plausible mechanism for the initial stages of the reaction involves a nucleophilic attack on TIBE from a carboxylate ion (–COO⁻) of MAH. The formation of the carboxylate ion could be catalyzed by water in the solvent or air. The attack facilitates the removal of isopropoxide groups because they are better leaving groups than ethyl acetoacetate.²³ The subsequent decomposition of the anhydride structure forms Ti–OOC– and –COO⁻ structures that could be responsible for the peak at 1730 cm⁻¹.

(19) Schmidt, H. K.; Oliveira, P. W.; Krug, H. *Mater. Res. Soc. Symp. Proc.* Coltrain, B. K., Sanchez, C., Schaefer, D. W., Wilkes, G. L., Eds. **1996**, 435, 13–23.

(20) Förster S.; Antonietti, M. *Adv. Mater.* **1998**, 10, 195–217.

(21) Léaustic, A.; Babonneau, F.; Livage, J. *Chem. Mater.* **1989**, 1, 240–247.

(22) Nakamoto, K. *Infrared and Raman Spectra of Inorganic and Coordination Compounds*, 4th ed.; John Wiley and Sons: New York, 1988; p 249.

(23) Léaustic, A.; Babonneau, F.; Livage, J. *Chem. Mater.* **1989**, 1, 248–252.

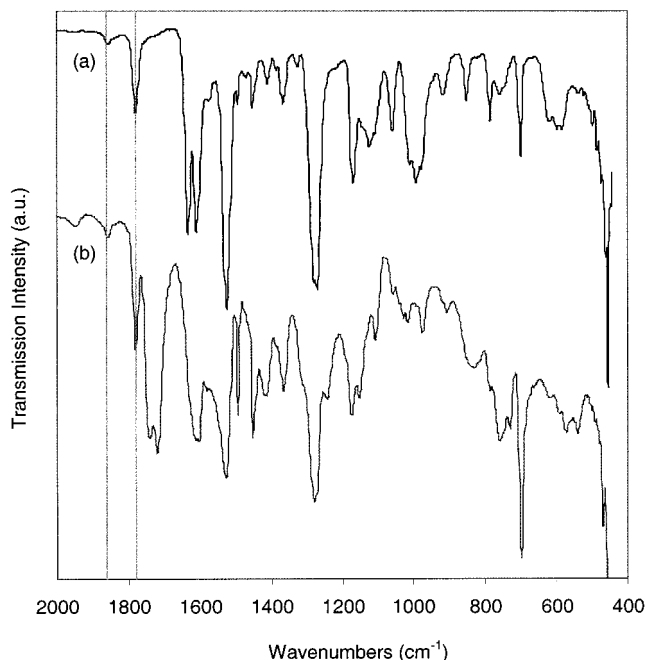


Figure 3. FTIR spectra of a 60/40 TIBE/S-MAH precursor solution (a) before and (b) gel formation. Lines indicate the presence of cyclic anhydride carbonyls after gel formation.

Further evidence of bonding between the TIBE and S-MAH is a minimum ratio of TIBE to MAH required to form crystalline BaTiO_3 particles. When films from precursor solutions of 80 and 90 wt % TIBE relative to S-MAH ($[\text{TIBE}]/[\text{MAH}] = 6.6$ and 14.9 , respectively) were reacted in aqueous $\text{Ba}(\text{OH})_2$, crystalline BaTiO_3 was observed by X-ray diffraction and TEM. In contrast, no crystalline BaTiO_3 was observed in films processed from solutions containing 60 wt % TIBE relative to S-MAH ($[\text{TIBE}]/[\text{MAH}] = 2.5$). However, crystalline BaTiO_3 has been observed in TIBE/SBS films with 50 wt % TIBE and lower.³ This suggests that all of the TIBE was covalently bound to MAH groups in S-MAH and that an excess of TIBE relative to MAH is obtained somewhere between $[\text{TIBE}]/[\text{MAH}]$ of 2.5 and 6.6. To calculate the concentration of TIBE sufficient to saturate the MAH sites, the stoichiometry of the reaction between TIBE and MAH would need to be determined. As with higher TIBE content films, FTIR spectra of the 60 wt % TIBE precursor also exhibited new peaks in the region $1720\text{--}1730\text{ cm}^{-1}$ (see Figure 3). However, the cyclic anhydride carbonyl peaks were still present, suggesting that MAH sites were still available for reaction. Moreover, when SBS in the same proportion was substituted for S-MAH, BaTiO_3 was observed via X-ray diffraction and TEM. This suggested that TIBE that was covalently bonded to S-MAH was unavailable to react with $\text{Ba}(\text{OH})_2$. Once the reactive MAH sites reached saturation, excess TIBE could be accommodated in the MAH block because the bound TIBE increased the miscibility of TIBE in S-MAH. This accounts for the uniform dispersion of BaTiO_3 nanoparticles observed for

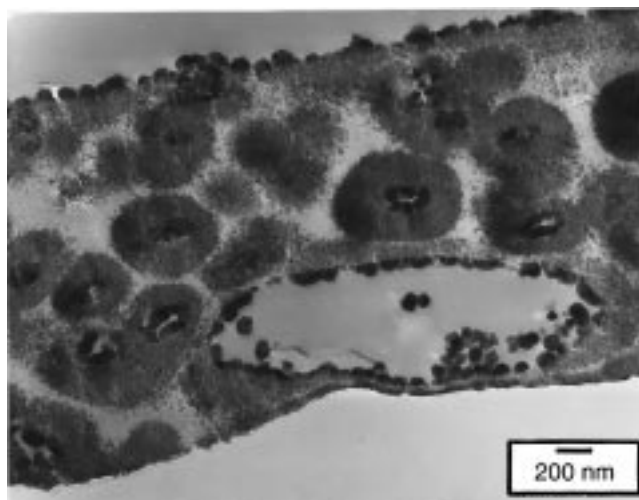


Figure 4. A different area of the BaTiO_3 /S-MAH composite film shown in Figure 1b.

precursor solutions with 90 wt % TIBE (Figure 1b).

Because S-MAH block copolymers are amphiphilic, they tend to form micelles in their equilibrium configuration, particularly in solvents such as toluene that have similar structural features to one of the blocks. Evidence of this behavior was observed in the same microtomed section as shown above (Figure 1b). BaTiO_3 formed in spherical domains (Figure 4), indicating that the TIBE preferentially segregated into the MAH block.^{20,24–27} This influence can also be seen in Figure 1b as arched structures in the film interior. Nonequilibrium effects such as varying rates of solvent evaporation in the film may have contributed to the variation in film microstructure. However, the specific processing conditions leading to the different morphologies were not investigated. The larger BaTiO_3 particles located at micelle centers as well as on film surfaces (Figures 1 and 4) are examples of particle growth freed from the constraints of the polymer matrix. For excess TIBE incorporated in the matrix (i.e., the MAH block), particle growth was physically constrained. However, particle growth in the micelle center continued until the local concentration of TIBE was exhausted.^{6,28–29}

Acknowledgment. We are indebted to Deb Van Horne and the Purdue School of Veterinary Medicine for use of their TEM preparation facilities. This research was funded by the Purdue Research Foundation and the National Science Foundation (contract DMR-9623744).

CM990349P

- (24) Clay, R. T.; Cohen, R. E. *Supramol. Sci.* **1995**, *2*, 183–191.
 (25) Sohn, B. H.; Cohen, R. E. *Acta Polym.* **1996**, *47*, 340–343.
 (26) Spatz, J.; Mössner, S.; Möller, M.; Kocher, M.; Neher, D.; Wegner, G. *Adv. Mater.* **1998**, *10*, 473–475.
 (27) Lee, T.; Yao, N.; Aksay, I. A. *Langmuir* **1997**, *13*, 3866–3870.
 (28) Chien, A. T.; Speck, J. S.; Lange, F. F.; Daykin, A. C.; Levi, C. G. *J. Mater. Res.* **1995**, *10*, 1784–1789.
 (29) Eckert, J. O.; Hung-Houston, C. C.; Gersten, B. L.; Lencka, M. M.; Riman, R. E. *J. Am. Ceram. Soc.* **1996**, *79*, 2929–2939.